IEIE Transactions on Smart Processing and Computing, vol. 6, no. 3, June 2017
https://doi.org/10.5573/IEIESPC.2017.6.3.141

A Novel Imaging System for Removal of Underwater Distortion using Code V

Vivek Maik, Stella Daniel, and A. Chrispin Jiji

[1] Department of Electronics and Communication, The Oxford College of Engineering, Bangalore, India
{vivek5681, stella.daniel997, chrispinjijipanjij}@gmail.com

***** Corresponding Author: Vivek Maik

Received January 3, 2017; Revised March 13, 2017; Accepted March 24, 2017; Published June 30, 2017

** Regular Paper*

** Invited Paper: This paper is invited by DonggyuSim, the associate editor.*

** Review Paper: This paper reviews the recent progress possibly including previous worksin a particular research topic, and has been accepted by the editorial board through the regular reviewing process.*

** Extended from a Conference: Preliminary results of this paper were presented at the IEEE VTC Fall 2012. This present paper has been accepted by the editorial board through the regular reviewing process that confirms the original contribution.*

***Abstract*:** Images obtained from underwater are usually degraded due to the environmental conditions. Some of the typical degradation factors include turbidity and color degradation. These degradations can be attributed to the absorptive and scattering properties of underwater degradation in terms of optical parameters, such as modulation transfer function (MTF), optical transfer function (OTF),point spread function (PSF), and color constancy. In this paper, we use the CODE V optical simulation software to mimic underwater conditions and model the imaging platform, thereby studying various parameters, such as PSF and MTF, and we use the PSF to remove the underwater turbidity. Experimental results show increased performance with the algorithm, compared to other existing methods.

***Keywords*:** CODEV, PSF, Turbidity

1. Introduction

Image processing algorithms have found increased usage in many applications, such as medical imaging, military defense, security, consumer electronics, etc. In this paper, we use image processing to remove underwater turbidity in images. Visibility in underwater images is usually hazy, but having a large number of individual particles in the water causes cloudiness or more haziness, called turbidity, which causes blur in underwater images. In order to remove any blur, we usually use blind deconvolution with an estimated or known PSF matrix:

$$x = H^{-1} y \tag{1}$$

where x is the restored clear image, H is the PSF kernel, and y is the turbid image. The main challenge is estimating the blur kernel [1-5]. The blur kernel cannot be estimated directly as it varies depending on the blur itself.

Existing methods use some form of prior to model the blur and, thereby, estimate the point spread function (PSF) for restoration of the underwater blurred images. Finally, because the amount of light is reduced when we go deeper, colors drop off one by one, depending on their wavelengths.

In this paper, in order to deal with underwater imaging, we address this problem from two different points of view:

I. the study of underwater distortion as an optical parameter
II. an image restoration technique for enhancement using an estimated optical parameter

Image restoration is viewed from an image formation point of view. We use optical imaging to learn the cause and characteristics of blur. An optical simulation will be used to mimic the conditions underwater, which in turn, will help us model the blur matrix, or PSF matrix. The main advantage of post-processing compared to pre-processing is that with post-processing, we only deal with

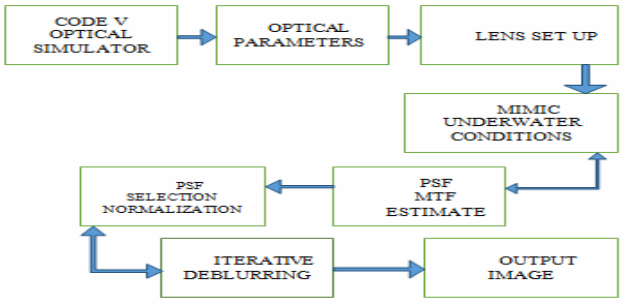

Fig. 1. Block diagram of the proposed method.

a PSF matrix, whereas the other characteristics of underwater images, like attenuation, refractive index, diffraction, and depth estimation can be ignored.

In Section 2, we briefly review the optical properties of underwater images. Section 3 explains the proposed algorithm, while Section 4 discusses enhancement of deblurred images, and Section 5 looks at color constancy. Section 6 presents the experimental results performance, and Section 7 concludes the paper.

2. Behaviour of Light in the Water

In this section, we will see how light behaves in water. Light in water as a medium is the same as air as a medium, it undergoes absorption and scattering mechanisms. Absorption is the loss of power as light travels in the medium, and scattering refers to deflection from a straight-line propagation path. In the underwater environment, light also undergoes diffraction and refraction because the wavelength and refractive index of water is different from air.

According to the Lambert-Beer empirical law, the decay of light intensity is related to the properties of the material via exponential dependence:

$$E(r) = E(0)e^{-cr} \tag{2}$$

where c is the total attenuation coefficient of the medium. The exponential coefficient measures combined light loss in the water. Typical attenuation coefficients for deep ocean water, coastal water, and bay water are 0.05m^{-1}, 0.2m^{-1}, and 0.33m^{-1}, respectively.

Total light loss, which is due to scattering and absorption coefficients, can be repeated as separate coefficients in a homogeneous isotropic medium:

$$E(r) = E(0)e^{-ar}e^{-br} \tag{3}$$

Another representation of light behavior in water can be seen as the sum of all the area in all angles through the volume scattering function with the angle of deviation from its direction of propagation using the below assumption and approximation of light in water.

$$b = 2\pi\int_0^{\pi}\beta(\theta)\sin\theta d\theta \tag{4}$$

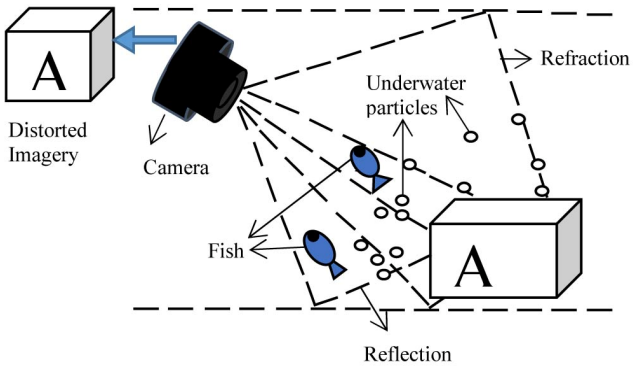

Fig. 2. Underwater imaging system.

However, these behaviors are complex, and always depend on location and angle parameters in water. Therefore, a proper mathematical model is needed to mimic the underwater conditions.

McGlamery[1] formed the theoretical foundations for the optical image formation model, while Jaffe [2] extended the model for designing different underwater image acquisition systems [1, 2].

Modeling of underwater imaging using statistical Monte Carlo techniques has also been proposed [3]. In this model, the underwater image can be represented as the linear trace of a light source from under the water to the camera. The light received by the camera consists of three components: (i) light reflected by an object with scattering, (ii) light reflected by an object without scattering, (iii) the back scatter component, L_B.

$$L_C = L_R + L_W + L_B \tag{5}$$

Next, we have to consider attenuation of light in order to model illumination under water. This attenuation needs to be included in water as the product of incident illumination and reflected light. The reflector surface model is assumed to be Lambertian, and geometric optics is used to compute the image of direct components in the camera plane. Now, this can be modeled on an optical imaging platform (CODE V). The optical imaging platform can be used to study the underwater imaging conditions and make the camera model with a PSF, a modulation transfer function (MTF), and Nyquist conditions.

3. Image Restoration using PSF Priors

The proposed approach approximates the underwater image as a linear system [8]. Image restorations do help in recovery of the original image f(x, y). A sharp image to be recovered from an underwater image using the PSF prior is estimated by CODEV as follows:

$$f(x,y) = h(x,y) * g(x,y) \tag{6}$$

where $h(x,y)$ represents the PSF prior, and $g(x,y)$

represents the turbid underwater image. And * denotes the convolution. The degradation function $h(x,y)$ needs to include the effects of the medium in this case. The whole process can be implemented in the frequency domain to eliminate convolution and replace it with multiplication:

$$F(u,v) = H(u,v).G(u,v) \tag{7}$$

Here, *H(u,v)*, the degradation, can be modeled as a product of degradation from the water medium, the optical system, and the depth of the water:

$$H(u,v) = PSF_{depth}.PSF_{\substack{water\\medium}}.PSF_{\substack{optical\\system}} \tag{8}$$

The better the information we have about the degradation function, the better the results of restoration. However, in underwater imaging, since the number of unknowns is due to multiple sources, we have to incorporate underwater optical properties in the PSF. In order to achieve this, we use three types of PSF to model the underwater imaging phenomenon:

$$H_{\substack{under\\water}} = PSF_{depth}.PSF_{\substack{spatial\\domain}}.PSF_{\substack{water\\scatter}} \tag{9}$$

$H_{\substack{under\\water}}$ can be modeled as a Gaussian symmetrical function given as

$$PSF_{\substack{water\\scatter}} = \exp\left\{-S(\varnothing)r\right\} \tag{10}$$

where $S(\varnothing)$ is the decay transfer function obtained for sea water conditions:

$$S(\varnothing) = \frac{c - b(1-\exp\{-2\pi\theta_0\varnothing\}}{2\pi\theta_0\varnothing} \tag{11}$$

where θ_0 is the mean angle, and b and c are the total scattering and attenuation coefficients, respectively.

The camera lens response can be measured for various values of θ_0, b, and c, and from these calibrated parameters, we can model the underwater PSF using CODEV. Using the PSF obtained from the above process, we can model an automated image restoration framework using a deconvolution filter.

In this paper, we propose a self-tuning automatic restoration filter that is based on a constrained minimization approach using directional regularization (CMADR).If the blur kernel is unknown; we face single-channel blind deconvolution, which is a class of imaging inverse problem. Past algorithms usually worked only for special cases, such as astronomical imaging, medical imaging, etc

The proposed CMARDR algorithm is formulated in the spatial domain and applied in the frequency domain.

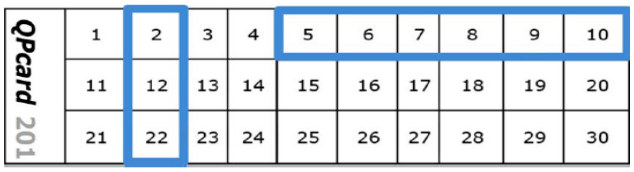

Fig. 3. QP card patches. Patches 2, 12, and 22 represent the reference R, G, and B colors, and patches 5–10 represent the reference gray levels for Tone Reproduction Curves.

$$F = H\,.\,G \tag{12}$$

The CMADR approach solves the above equation for H and G by adopting some form of regularization; formally, this leads to a constrained optimization problem and can be represented as

$$arg\min_{G,H}\{F\} + \lambda\left\{\nabla_x^2 + \nabla_y^2\right\} + Q(G) \tag{13}$$

The above expression represents the CMADR process, which has λ as the regularization term. $\nabla_x\nabla_y$, as the gradient information of image F and Q (G), represent the Bregman iteration for additional smoothing. The above minimization can be done iteratively with multiple minimizations.

The iterations first minimize for H, and then they minimize for G. By doing it this way, we can minimize for least square approximation:

$$\min_G \frac{\gamma}{2}GH - F^2 + \lambda\left(D_xG + D_yG\right) \tag{14}$$

where γ is the regularization parameter, and D_x and D_y are directional gradients.

By applying variable splitting, we replace D_xG with V_x and D_yG with V_y. The above problem now becomes constrained optimization:

$$\min_{G,V_x,V_y} \frac{\gamma}{2}GH - F^2 + \lambda\left(V_xV_y\right) \tag{15}$$

The above augmented Lagrangian method (ALM), or split Bregman iteration, tackles the constrained problem in a two-step iterative process.

4. Image Enhancement of Deblurred Images

The deblurred image is subject to global enhancement with no prior required. This is necessaryto reduce the architects due to deblurring, and for the enhancement of color information otherwise degraded in the underwater image formation process. Different depth levels allow different colors to be distorted. As a consequence, faded and non-uniform color distribution will characterize the

Fig. 4. Gretage Macbeth Profile checker card.

underwater image. Mauricio [20, 21] proposed an algorithm to readily preprocess the underwater imaging using homomorphic filtering, wavelet de-noising anisotropic filtering, and RGB color channel equalization to enhance faded color. The algorithm is automatic and requires no prior or parameter adjustment. Another such method uses distribution of the histogram to make the bins change according to color density.

In the proposed work, we use a color chart maker (QP card), shown in Fig. 4. Comparing the image colors with the chart color, the color correction matrix can be obtained as

$$M_{XYZ} = M_{chart} M^{1}_{RGB} \tag{16}$$

Using singular value decomposition (SVD), the above matrices can be written as

$$M_{XYZ} = \begin{pmatrix} X_1 & X_2 ..... & X_N \\ Y_1 & Y_2 ..... & Y_N \\ Z_1 & Z_2 ..... & Z_N \end{pmatrix} \tag{17}$$

$$M_{chart} = \begin{pmatrix} m_{11} & m_{12} & m_{13} \\ m_{21} & m_{22} & m_{23} \\ m_{31} & m_{32} & m_{33} \end{pmatrix} \tag{18}$$

$$M^{1}_{RGB} = \begin{pmatrix} R'_1 & R'_2 ..... & R'_N \\ G'_1 & G'_2 ..... & G'_N \\ B'_1 & B'_2 ..... & B'_N \end{pmatrix} \tag{19}$$

The arrangement using SVD gives

$$\begin{pmatrix} X_1 \\ X_2 \\ . \\ . \\ . \\ X_n \end{pmatrix} = \begin{pmatrix} m_{11} \\ m_{12} \\ m_{13} \end{pmatrix} \tag{20}$$

$$\begin{pmatrix} Y_1 \\ Y_2 \\ . \\ . \\ . \\ Y_n \end{pmatrix} = \begin{pmatrix} R_1 & G_1 & B_1 \\ R_2 & G_2 & B_2 \\ . & . & . \\ . & . & . \\ . & . & . \\ R_N & G_N & B_N \end{pmatrix} \begin{pmatrix} m_{11} \\ m_{12} \\ m_{13} \end{pmatrix} \tag{21}$$

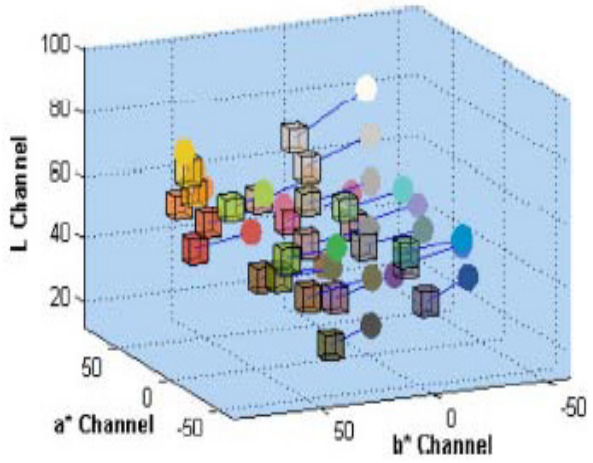

Fig. 5. Color difference between QP card colors in a T source image and the reference chart. The color difference for white point location is used in computing the color mixture map, which is used to fuse T, F, and P source images.

As can be seen above, the chart colors equalize the color contrast in the image. Secondly, the International Color Consortium (ICC) profile space of the color corrected image is compared with the standard profile space.

5. Color Constancy

Color constancy algorithms are, for the most part, constructed in view of the improving suspicion that ghastly dispersion of a light source is uniform, crosswise, between scenes. However, in reality, this assumption is often correct due to the presence of multiple light sources.

The steps in color correction systems for images illuminated by multiple light sources are as follows.

- Input image capture.
- Two light sources and reference QP card.
- Estimation of color correction matrix and tone reproductive curves.
- Modifying ICC profile tags to generate United Development -Profile Correction System.
- Color mixture map extraction for fusion of input source image.
- Fusion of color-corrected image.
- Output image.

Pictures in the proposed technique are isolated into patches, which are thought to be sufficiently little, such that it is predictable with the uniform otherworldly supposition. For every patch, illuminant estimation is acquired by utilizing a standard color steadiness calculation (assuming a uniform light source).

Numerous light-source assessments can be all the while considered, yet in this paper, the attention is on single assessments per patch. Since the utilized calculations simply assess the chromaticity of the light source, each appraisal is standardized for power, i.e,

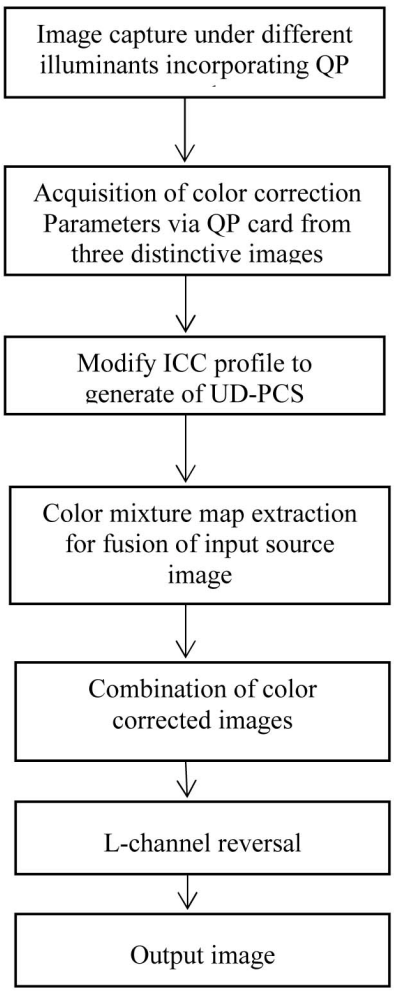

Fig. 6. Algorithm for color constancy.

$$\begin{Bmatrix} r = R/(R+G+B) \\ g = G/(R+G+B) \end{Bmatrix} \quad (21)$$

The illuminant over every patch is spoken to by a 1*2 vector. A hypothetical circumstance could happen where the illuminant gauge results in a dark light source. In such circumstances, though improbable, we propose utilizing a white-light source, i.e. r=g=1/3.

5.1 Image Capture and Estimation of Color Adjustment Parameters

The meaning of T, F, and P, is shown in the table below, and each image was obtained using tungsten, fluorescent, and mixed light sources. Generation of T, F, and P images using T and F light sources, and estimation of differences in colors caused by each light source is shown below in the Fig. 8.

6. Experimental Result and Performance

In this experimental result and performance technique,

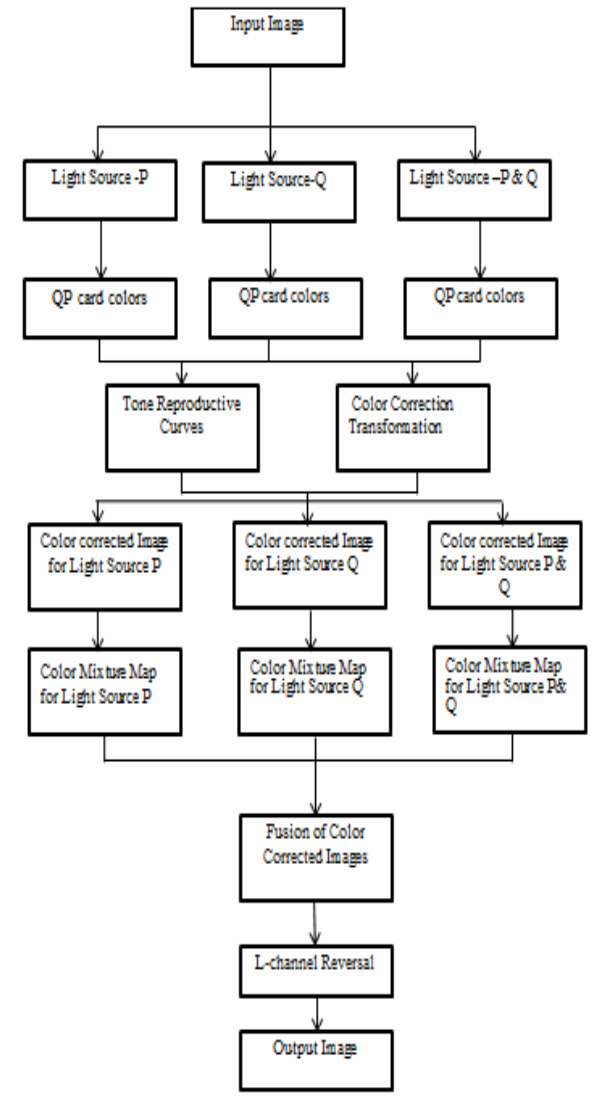

Fig. 7. Block diagram of the color correction system.

there are three steps.

- Use CODE V to find the PSF of the image.
- After finding a PSF of the image, use deblurred code to find the original image.
- If the original image has a lighting problem, use a color-correction method to find the clear image.

This is actually a process that takes place inside the CODE V software to estimate PSF. Once the PSF is estimated in CODE V, it is then implemented using Matlab to provide an effective and efficient method to reconstruct the original image. In Matlab, the estimated PSF is considered blur, and is added to the original image to make it blurry, and is then added with Gaussian noise to get a blurred noisy image. The blurred noisy image is subjected to a blind deconvolution method, which recovers the original image free from blur and noise.

For example, we considered a microscope lens for which a PSF was estimated, and the same was used for implementation in Matlab to recover the original image.

At first, when we select the type of lens for which the PSF has to be calculated, CODE V shows the image of that

Table 1. Technical terminologies for different images and profiles.

Notions	Meaning
Tungsten (T) image	Image obtained using tungsten light source
Fluorescent (F) image	Image obtained using fluorescent light source
Pseudo (p) image	Image obtained using mixed tungsten and fluorescent light sources
T, F ,and P Profiles	Tungsten, fluorescent, and pseudo color profiles respectively
T and F Sources	Tungsten and fluorescent, light sources respectively
P source	Mixed tungsten and fluorescent light sources
T and F-stop	Exposure setting for tungsten and fluorescent light sources, respectively

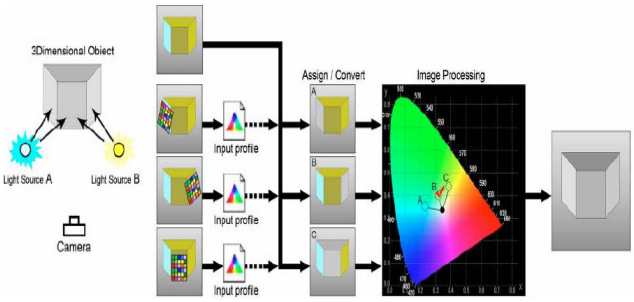

Fig. 8. Block diagram of the proposed color constancy algorithm, which illustrates step-by-step functional flow from left to right.

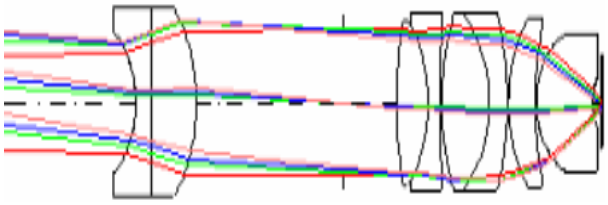

Fig. 9. Microscope lens.

particular lens, as shown in Fig. 9.

When the PSF matrix is calculated by CODE V, then this matrix is implemented in Matlab to perform the deconvolution process. While considering the PSF matrix, we mainly concentrated on the center-most portion of the matrix, because it has a high value, indicating more volume of blur, and the surrounding values are a little less (compared to the middle), indicating less blur. So, while calculating the blur (PSF), we should mainly concentrate on the center-most portion, so we can remove the blur completely.

Along with the PSF matrix, CODE V also displays a graphical representation of the PSF and its color plot, which is clearly shown in the following Figs. 10 and 11.

A comparison in the region of color gradients or

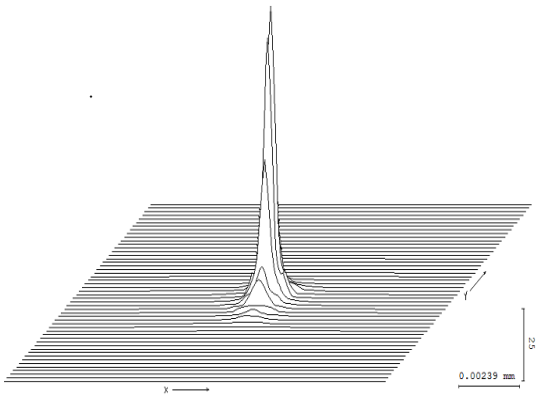

Fig. 10. Graphical plot of the PSF.

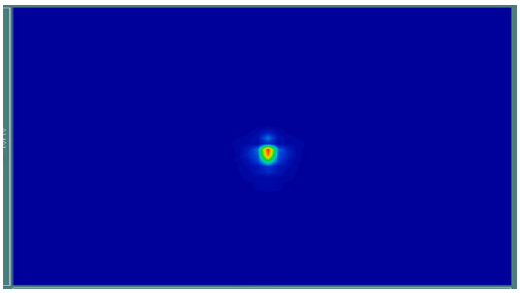

Fig. 11. Color plot of the PSF.

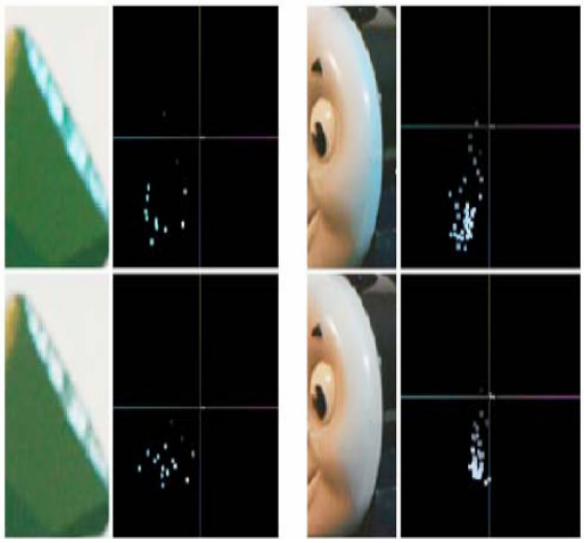

(a) (b)

Fig. 12. Color scatter plot at specific regions of the image. The upper images in (a) to (b) represent the scatter plot of the original P image, and the lower images show the difference after the color constancy algorithm has been applied.

transition is in Fig. 12. Fig. 13 shows the tested image and the constructed image using the color constancy method.

Finally, we use deblurred code to find the reconstructed image, and after we finish deblurring the image, we then used the color constancy method to improve the image.

Fig. 13. Experimental results on Hat, Parrot, and Bike.

Table 2. Comparisons of different parameter values.

Parameters / Images	Original image values and average proposed methodologies image values			Reconstructed image values of:		
	PSNR	RMSE	SSIM	PSNR	RMSE	SSIM
PARROTS	23.87	16.32	1.50	31.33	14.30	0.90
HAT	25.73	13.17	1.29	31.80	11.10	0.87
BIKE	17.76	15.04	1.02	23.76	14.10	0.95
FLOWER	28.42	14.05	1.33	34.45	12.05	0.85
BUTTERFLY	29.77	14.06	1.45	34.45	13.05	0.88
RACCON	24.66	15.5	1.34	31.65	13.04	0.88
ANIMAL	16.52	10.09	1.05	22.69	9.04	0.89

Images Name	Original Images	Original Image With Noise	Reconstructed Image
PARROTS		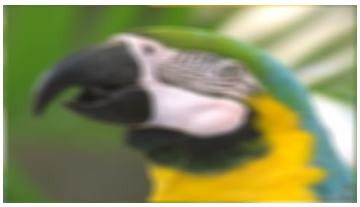	
HAT			
BIKE		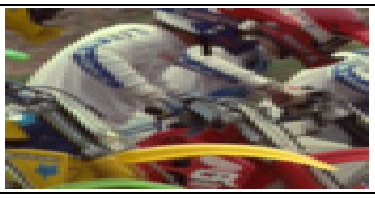	
FLOWER			
BUTTERFLY	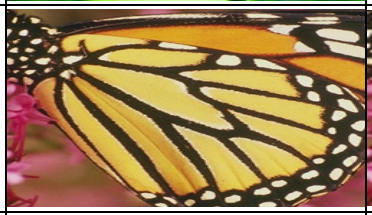	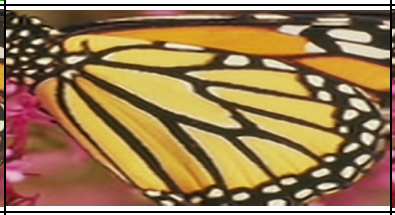	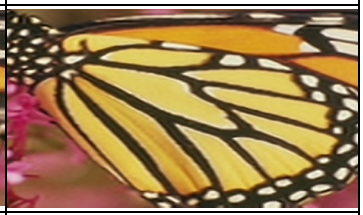
LIONCUB			
ANIMAL			

Fig. 14. Comparison between blurred images and reconstructed images.

7. Conclusions

We proposed a novel underwater representation-based CODE V and image deblurring method using adaptive sparse domain selection (ASDS) and a color constancy methodology. Considering the fact that underwater images can vary significantly across different images and different image patches in a single image, in this paper, we use the above three techniques to improve the image, in that we first use CODEV to find the PSF of the original image (the blurred image), and second, we adaptively select the dictionaries that were pre-learned from a dataset of high-quality example patches for each local patch. ASDS significantly improves the effectiveness of underwater modeling, and consequently, the results of image restoration.

The experimental results on natural images showed that the proposed ASDS approach outperforms many state-of-the-art methods in both peak signal-to-noise ratio and visual quality. Finally, we use a constancy method to clear the lighting (color) in state-of-the-art images.

References

[1] B. McGlamery, "A computer model for underwater camerasystem," in *Ocean Optics VI*, S. Q. Duntley, Ed., vol. 208 of *Proceedings of SPIE*, pp. 221–231, 1979.

[2] J. S. Jaffe, "Computer modeling and the design of optimal underwater imaging systems," *IEEE Journal of Oceanic Engineering*, vol. 15, no. 2, pp. 101–111, 1990.

[3] C. Funk, S. Bryant, and P. Heckman, "Handbook of underwater imaging system design," Tech. Rep. TP303, Naval Undersea Center, San Diego, Calif, USA, 1972.

[4] T. H. Dixon, T. J. Pivirotto, R. F. Chapman, and R. C. Tyce, "A range-gated laser system for ocean floor imaging," *Marine Technology Society Journal*, vol. 17, 1983.

[5] J.McLean and K. Voss, "Point spread functions in ocean water: comparison between theory and experiment," *Applied Optics*, vol. 30, pp. 2027–2030, 1991.

[6] K. Voss, "Simple empirical model of the oceanic point spread function," *Applied Optics*, vol. 30, pp. 2647–2651, 1991.

[7] J. Jaffe, K. Moore, J. McLean, and M. Strand, "Under water optical imaging: status and prospects," *Oceanography*, vol. 14,pp. 66–76, 2001.

[8] J. Mertens and F. Replogle, "Use of point spread and beam spread functions for analysis of imaging systems in water," *Journal of the Optical Society of America*, vol. 67, pp. 1105– 1117, 1977.

[9] W. Hou, D. J. Gray, A. D. Weidemann, G. R. Fournier, andJ. L. Forand, "Automated underwater image restoration and retrieval of related optical properties," in *Proceedings of the IEEE International Geoscience and Remote Sensing Symposium (IGARSS '07)*, pp. 1889–1892, 2007.

[10] W. Hou, A. D. Weidemann, D. J. Gray, and G. R. Fournier, "Imagery-derived modulation transfer function and its applications for underwater imaging," in *Applications of Digital Image Processing*, vol. 6696 of *Proceedings of SPIE*, San Diego, Calif, USA, August 2007

[11] Bartolini, L., De Dominicis, M., Ferri de Collibus, G., Fornetti, M., Guarneri, E., Paglia, C.P. and Ricci, R. 2005. Underwater three-dimensional imaging with an amplitude- modulated laser radar at a 405 nm wave-length. Appl Opt. 44:7130-7135.

[12] Baumgartner, L., Reynoldson, N., Cameron, L. and Stanger, J. 2006. Application of a dual-frequency identification sonar (DIDSON) to fish migration studies.

[13] In: Lyle, J.M., Furlani, D.M. and Buxton, C.D., eds. Cutting-edge technologies in fisheries science. Australian SocForProc Fish Biology Wkshp Proc., 91-98.

[14] Benzie, P.W., Watson, J., Burns, N., Sun, H.Y. 2007a. Developments for underwater remote vision. IEEE 3DTV Conference, Kos, Greece, 1-4.

[15] Blevins, E. and Johnsen, S. 2004. Spatial vision in the echinoid genus Echinometra. J Exp Biol. 207:4249-4253.

[16] RaimanodoSchettini and Silvia Corchs "Underwater Image Processing: State of the Art of Restoration and Image Enhancement Methods", *EURASIP Journal on Advances in Signal Processing*,2010.

[17] Code V reference manual.

[18] Z.Liu, Y.Yu, K.Zhang and H.Huang, "underwater image transmission and blurred image restoration," *opticalEngineering,* vol.40,no6, pp 1125-1131,2001.

[19] B. McGlamery, "A computer model for underwater camera system," in *Ocean Optics* VI, S. Q. Duntley, Ed., vol. 208 of Proceedings of SPIE, pp. 221–231, 1979.

[20] Mauricio Delbracio, Publo Muse , Andres Almansa "Non –parametric Sub – Pixel Local Point Spread Function Estimation," *Image Processing online*, 2012.

[21] Y. Y. Schechner and N. Karpel, "Recovery of underwater visibility and structure by polarization analysis," *IEEE Journal of Oceanic Engineering, vol.* 30, no. 3, pp. 570–587, 2005.

Vivek Maik received his B tech degree in Electronics and communication at Cochin University. He received Masters and PhD in Image Processing from Chung-Ang University (CAU) Seoul, Korea, in 2010. Currently, he is serving as Associate Professor in Electronics & Communication at the University of VTU, Karnataka, India. Before starting his professor carrier, he worked at the Korea Samsung Electronics as an assistant researcher. He was involved in various projects including lenses, semiconductor chips. His research interests include sparse representation, Image Deblurring, Super resolution, Reranking and many. He is guiding many PhD students. He has been awarded a gold medal for the best paper presented in ICCE- Asia, International conference- 2016.

A. Chrispin Jiji received the B.E degree in Electronics and communication engineering from Manonmanium Sundaranar University, Thirunelveli in 2004 and M.E degree in Applied Electronics from Karunya Deemed University, Coimbatore in 2006 respectively. Currently, she is pursuing the Ph.D. degree in Electrical Engineering at Visvesvaraya Technological University, Belgaum, Karnataka and working as Assistant Professor in The Oxford College of Engineering, Bangalore, Karnataka. Her current research area is Image Processing.

Stella Daniel received B.E degree in Electronics and communication engineering from Loyola Institute of Technology, Chennai in 2014 and currently Pursuing M. Tech degree in VLSI Design and Embedded Systems from The Oxford College of Engineering, Bangalore. She is working in the image processing domain under the guidance of Dr. Vivek Maik.